Journal of Translational Medicine

RESEARCH

Open Access

Interleukin-1β mediates a tumor-supporting environment prompted by IGF1 in triple-negative breast cancer (TNBC)

Domenica Scordamaglia[1†], Marianna Talia[1†], Francesca Cirillo[2], Azzurra Zicarelli[2], Adelina Assunta Mondino[1], Salvatore De Rosis[1], Marika Di Dio[1], Francesca Silvestri[1], Chiara Meliti[1], Anna Maria Miglietta[3], Carlo Capalbo[1,4], Ernestina Marianna De Francesco[2], Antonino Belfiore[5], Marcello Maggiolini[1*] and Rosamaria Lappano[1*]

Abstract

Background The intricate mechanisms that associate obesity with triple-negative breast cancer (TNBC) remain to be disclosed. Considering that obesity is linked with an increased bioavailability of the insulin-like growth factor 1 (IGF1), we evaluated whether IGF1 triggers aggressive features in TNBC cells and the molecular paths involved.

Methods Gene expression and Chromatin Immunoprecipitation experiments, ELISA, immunoblotting, immunoprecipitation and immunofluorescence assays, combined with two-dimensional and three-dimensional in vitro model-based studies, were used to investigate the molecular mechanisms through which IGF1 may promote proliferative and motile responses in TNBC cells and reprogram normal fibroblasts into cancer-associated fibroblasts (CAFs)-like cells. The translational relevance of the results obtained was supported by bioinformatics analyses leveraging data from extensive TNBC patient databases.

Results We found that the cytokine interleukin-1β (IL-1β) mediates certain IGF1 actions within the tumor microenvironment, hence facilitating the TNBC landscape. Mechanistically, we assessed that the IGF1/IGF1 receptor (IGFIR) axis induces the collagen VI-dependent activation of discoidin domain receptor 1 (DDR1) and the subsequent increase of the G protein estrogen receptor (GPER), toward IL-1β regulation and secretion. Consequently, IL-1β promoted both the autocrine stimulation of TNBC cells and the differentiation of normal fibroblasts into cancer-associated fibroblasts (CAFs)-like cells, which in turn achieved a proliferative profile and enhanced the motility of TNBC cells.

Conclusions IL-1β may be considered as a therapeutic target in more comprehensive approaches in obese TNBC patients exhibiting high IGF-1 bioavailability.

Keywords Interleukin 1β (IL1β), Triple-negative breast cancer (TNBC), Cancer associated fibroblasts (CAFs), Insulin-like growth factor 1 (IGF1), Discoidin domain receptor 1 (DDR1), G protein estrogen receptor (GPER)

[†]Domenica Scordamaglia and Marianna Talia Authors contributed equally to this work

*Correspondence:
Marcello Maggiolini
marcello.maggiolini@unical.it
Rosamaria Lappano
rosamaria.lappano@unical.it
Full list of author information is available at the end of the article

Background

Obesity is well recognized as a significant risk factor for the progression of breast cancer (BC) [1, 2]. Indeed, diverse metabolic alterations that characterize obesity, like insulin resistance, chronic inflammation and metabolic reprogramming, have been associated with BC worsening and spreading [3–7]. A relationship between obesity and aggressive BC subtypes, such as triple-negative breast cancer (TNBC), has also been reported, even though the underlying mechanisms remain to be fully understood [8]. Previous studies have suggested that high circulating levels of insulin-like growth factor 1 (IGF1) may play a role in the risk of BC development in obese women [9–13]. Increased levels of IGF1 and enhanced expression of the cognate receptor, namely IGF1R, are also correlated to poor BC outcomes in patients affected by TNBC [8, 14]. In this scenario, the activation of the IGF1/IGF1R signaling pathway is linked to multiple oncogenic events like proliferation, survival, migration, angiogenesis and epithelial to mesenchymal transition (EMT) in BC cells [15–20]. In addition, our previous studies have demonstrated that the IGF1/IGF1R axis engages a functional cooperation with both the collagen receptor, named discoidin domain receptor 1 (DDR1), and the alternate estrogen receptor, known as G Protein Estrogen Receptor (GPER), which are both known mediators of tumor progression [21–26].

The contribution of a pro-inflammatory tumor microenvironment (TME) in BC progression and therapy resistance has been largely acknowledged also in the context of obesity, insulin resistance and dysregulated insulin/IGF axis [27–30]. In particular, cancer-associated fibroblasts (CAFs) that are main players within the breast tumor stroma trigger multilayered communications with cancer cells through the secretion of a variety of molecules, including various cytokines [27, 31, 32]. In turn, the chemokine network influences many aspects of tumor progression like immune cell infiltration and cancer cell growth, survival, motility and angiogenesis [33].

Interleukin-1β (IL-1β) is an important pro-inflammatory cytokine involved in metastatic, angiogenic and immunosuppressive pathways leading to BC progression [34–36]. Noteworthy, IL-1β is frequently up-regulated in BC and correlates with pathologic features indicative of aggressive tumor behavior and poor prognosis [37, 38]. In this framework, our previous studies also demonstrated that IL-1β cooperates with GPER signaling, leading to proliferative and invasive responses in both TNBC cells and CAFs [34].

Here, we provide novel insights into the mechanisms through which IGF1 may facilitate TNBC progression. Specifically, we show the molecular paths mediating IL-1β expression and action upon IGF1 stimulation, therefore highlighting this cytokine as a promising target for novel therapeutic options in obese TNBC patients characterized by elevated IGF1 bioavailability.

Methods

Reagents

IGF1 was purchased from Merck (Milan, Italy). The MEK inhibitor trametinib, the IGF1R inhibitor OSI-906 and the IL1R1 antagonist raleukin were obtained from MedChemExpress (DBA, Milan, Italy). DDR1 tyrosine kinase inhibitor DDR1-IN-1 dihydrochloride was obtained by Tocris Bioscience (Bristol, UK). All compounds were dissolved in DMSO, except for IGF1 that was solubilized in water. Recombinant human IL-1β was purchased from Thermo Fisher Scientific (Thermo Fisher Scientific, Monza, Italy) and solubilized in PBS with 1% BSA.

Cell cultures

MDA-MB-231 and MDA-MB-436 breast cancer cells were obtained from ATCC (Manassas, VA, USA), used less than 6 months after resuscitation, and routinely tested and authenticated according to the ATCC suggestions. MDA-MB-231 and MDA-MB-436 cells were maintained in DMEM/F12 (Dulbecco's Modified Eagle Medium/Nutrient Mixture F-12) with phenol red, supplemented with 5% fetal bovine serum (FBS) and 1% penicillin/streptomycin (Thermo Fisher Scientific, Monza, Italy). Human embryonic lung fibroblasts (WI-38) were provided by ATCC (Manassas, VA, USA) and cultured in EMEM medium (Manassas, VA, USA) containing 10% FBS (Gibco, Carlsbad, CA, USA) and 1% penicillin–streptomycin (Thermo Fisher Scientific, Monza, Italy). All cells were grown in a 37 °C incubator with 5% CO2 and switched to medium without serum and phenol red or 5% charcoal-stripped FBS the day before treatments to be processed for experiments.

Bioinformatics analyses

Bioinformatics analyses were performed in R Studio (R version 4.4.1) using the publicly available dataset The Cancer Genome Atlas (TCGA) [39]. The clinical information and gene expression data (RNA Seq V2 RSEM) of the Invasive Breast Cancer Cohort of the TCGA project were retrieved from UCSC Xena (https://xenabrowser.net/). Samples of the TCGA cohort (n. 1247) were filtered by the "sample type" in order to obtain exclusive information on tumor tissues. Moreover, patients were filtered on the basis of the estrogen receptor (ER), progesterone receptor (PR) and human epidermal growth factor receptor 2 (HER2) in order to distinguish non-TNBC from TNBC (n. 123). Gene expression and clinical information were also filtered for missing values. Pearson correlation coefficients (r-values) were calculated using the R cor.

test function and setting the method as "Pearson". Scatter plots were assessed with the R tidyverse package. The statistical analyses were performed by using the t-test.

Survival analyses

Survival analyses were performed using the TCGA gene expression data along with the disease-free interval (DFI) information. The survivALL package was employed in R Studio to examine Cox proportional hazards for all possible points of separation (low–high cut-points), selecting the cut-point with the lowest p-value [40]. Therefore, patients were divided according to high and low expression levels of specified genes. The Kaplan Meier survival curves were generated using the survival and the survminer packages in R Studio.

Gene expression studies

Total RNA was extracted, and cDNA was synthesized by reverse transcription, as previously described [41]. The expression of selected genes was quantified by real-time PCR using the platform Quant Studio7 Flex Real-Time PCR System (Thermo Fisher Scientific, Monza, Italy). Gene-specific primers were designed using Primer Express version 2.0 software (Applied Biosystems). Assays were performed in triplicate and the results were normalized for actin beta (ACTB) expression and then calculated as fold induction of RNA expression. Gene-specific primers were designed using Primer Express version 2.0 software (Applied Biosystems) and are as follows: 5'-GCAACGACTACGCCACCAT-3' (COL6A2 forward) and 5'-CTTCGTGTTTCATGACCTTGATG-3' (COL6A2 reverse); 5'-TATGTGGCAATGCGTTCTCTA TCCA-3' (E-CADHERIN forward) and 5'-TGGAATCCA AGCAGAATTGC-3' (E-CADHERIN reverse); 5'-AGA AGAAAGCAGAACTGGATG-3' (FAP forward) and 5'-ACACACTTCTTGCTTGGAGGAT-3' (FAP reverse); 5'-TTAAAGCCCGCCTGACAGA-3' (IL-1β forward) and 5'-GCGAATGACAGAGGGTTTCTTAG-3' (IL-1β reverse); 5'-AAGCCACCCCACTTCTCTCTAA-3' (ACTB forward) and 5'-CACCTCCCCTGTGTGGAC TT-3' (ACTB reverse).

Plasmids and gene silencing experiments

Cells were transfected, as previously reported [42], using TurboFect™ Transfection Reagent (Thermo Fisher Scientific, Monza, Italy) for 36 h before treatments with a control vector (shRNA, pLKO.1-puro non-target shRNA) or a shGPER (TRCN0000235159, target sequence: TCT CGTGCCTCTACACCATCT) purchased from Merck (Milan, Italy). The overexpression of a kinase-inactive variant of DDR1 (DDR1/K618A), which encodes for a mutant DDR1 that is not phosphorylated upon collagen stimulation, was performed by transiently transfecting the cells for 48 h with either an empty vector (pCMV6-Entry vector) or the DDR1/K618A mutant cDNA using TurboFect™ Transfection Reagent (Thermo Fisher Scientific, Monza, Italy) according to the manufacturer's instructions. The DDR1 mutant K618A in the pCMV6-Entry vector (OriGene, Rockville, MD, USA) was generated with the QuikChange II XL Site-Directed Mutagenesis Kit (Agilent Technologies), as previously described [43]. For the transfection of the plasmid DN/c-fos (a kind gift from Dr. C. Vinson, NIH, Bethesda, MD, USA), which encodes for c-fos mutant that heterodimerizes with c-fos dimerization partners but does not allow DNA binding, cells were transfected using X-treme GENE 9 DNA Transfection Reagent (Roche Diagnostics, Merck, Milan, Italy) for 24 h before treatments. For siRNA experiments, cells were transiently transfected using Lipofectamine RNAiMax (Thermo Fisher Scientific, Monza, Italy) according to the manufacturer's instructions. For silencing DDR1, either the select predesigned pool of four siRNA oligos for 10 nM DDR1 (Human DDR1 siGENOME SMARTpool, M-003111–04) or a pool of four scramble siRNA oligos (Thermo Fisher Scientific Dharmacon. Waltham, MA, USA) were used.

Chromatin immunoprecipitation (ChIP) assay

Cells were grown in 10-cm dishes, exposed to treatments, and then cross-linked with 1% formaldehyde and sonicated. Supernatants were immuno-cleared with salmon DNA/protein A/G agarose (Merck, Milan, Italy) and immunoprecipitated with anti-c-fos antibody (E-8) (Santa Cruz Biotechnology, DBA, Milan, Italy) or nonspecific IgG. Pellets were washed, eluted with a buffer consisting of 1%SDS and 0.1 mol/L NaHCO3, and digested with proteinase K. DNA was obtained by phenol/chloroform extractions and precipitated with ethanol. The yield of target region DNA in each sample after ChIP assay was analyzed by real-time PCR. The primers used to amplify the region containing an AP-1 site located in the IL-1β promoter sequence were: 5'-CCTTCCCTCTCTGCC TCCC-3' (forward) and 5'-AACCTTTAGGGTGTCAGC TG-3' (reverse). Data were normalized to the input for the immunoprecipitation and the results were reported as fold changes respect to nonspecific IgG.

Western blot analysis

Cells were grown in 10-cm dishes, exposed to treatments, and then lysed as previously described [44]. Equal amounts of whole-protein extract were resolved on a 8 or 10% SDS–polyacrylamide gel and transferred to a nitrocellulose membrane (Merck, Milan, Italy), which were probed with primary antibodies against IL-1β (R&D Systems, Bio-Techne, Milan, Italy) COL6A2 (ab180855) and GPER (AB137479) (Abcam, DBA, Milan, Italy),

Phospho-Tyrosine (4G10) (96,215) and DDR1 (D1G6) (Cell Signaling Technology, Euroclone, Milan, Italy, phosphorylated ERK1/2 (E-4), ERK2 (C-14), c-fos (E-8) and β-actin (AC-15) (Santa Cruz Biotechnology, DBA, Milan, Italy). Proteins were detected by horseradish peroxidase-linked secondary antibodies (Bio-Rad, Milan, Italy) and then revealed using the chemiluminescent substrate for western blotting Clarity Western ECL Substrate (Bio-Rad, Milan, Italy). Western blot analysis was performed as described above.

Immunoprecipitation assay

After exposure to treatments, cells were washed and lysed using 500 µl RIPA buffer with protease inhibitors (1.7 mg/ml aprotinin, 1 mg/ml leupeptin, 200 mmol/l phenylmethylsulfonyl fluoride, 200 mmol/l sodium orthovanadate and 100 mmol/l sodium fluoride). Samples were then centrifuged at 13,000 rpm for 10 min and protein concentrations were determined using Coomassie (Bradford) protein assay. Proteins (250 µg) were then incubated for 2 h with immunoprecipitation buffer with inhibitors, 2 µg of anti-DDR1 antibody (D1G6) (Cell Signaling Technology, Euroclone, Milan, Italy), and 20 µl of Protein A/G agarose immunoprecipitation reagent (Santa Cruz Biotechnology, DBA, Milan, Italy). Samples were then centrifuged at 13,000 rpm for 5 min at 4 °C to pellet beads. Pellets were washed four times with 500 µl of PBS and centrifuged at 13,000 rpm for 5 min at 4 °C. Supernatants were collected, resuspended in 20 µl RIPA buffer with protease inhibitors, 2X SDS sample buffer and heated to 95 °C for 5 min. Samples were then run on 8% SDS-PAGE, transferred to nitrocellulose and probed with primary antibodies. Western blot analysis and ECL detection were performed as described above.

Immunofluorescence microscopy

WI-38 cells were grown on a coverslip, incubated in a medium containing 5% charcoal-stripped FBS and then cultured, in the presence or absence of 5 µg/ml IL1R1 antagonist raleukin, for 72 h with conditioned media collected from MDA-MB-231 cells previously treated with vehicle or 50 ng/ml IGF1. Alternatively, WI-38 cells were treated with vehicle or 10 ng/mL IL-1β for 72 h alone or in combination with 5 µg/ml IL1R1 antagonist raleukin, as indicated. Next, cells were fixed in 4% paraformaldehyde in PBS, permeabilized with 0.2% Triton X-100, washed 3 times with PBS and incubated at 4 °C overnight with the primary antibody (1:250) against fibroblast-activated protein (FAP) (H-56; Santa Cruz Biotechnology, DBA, Milan, Italy). After incubation, the slides were extensively washed with PBS, probed with Goat anti-Rabbit IgG (H + L) Cross-Adsorbed Secondary Antibody, Alexa Fluor™ 594 (1:300, Thermo Fisher Scientific, Milan, Italy) for 1 h at room temperature, washed three times with PBS and incubated for 3 min with 4′,6-diamidino-2-phenylindole dihydrochloride (DAPI) (1:10,000; Merck, Milan, Italy). Then, the images were obtained using the Cytation 3 Cell Imaging Multimode reader (BioTek, AHSI, Milan Italy) and analyzed by the Gen5 software (BioTek, AHSI, Milan Italy).

Enzyme-linked Immunosorbent assay (ELISA)

The concentrations of COL6A2 and IL-1β in supernatants from IGF1-treated MDA-MB-231 and MDA-MB-436 cells were measured using human COL6A2

(See figure on next page.)

Fig. 1 IGF1 induces the COL6A2-dependent activation of DDR1 along with the up-regulation of IL1-β in TNBC cells. mRNA (**A**) and protein (**B**) levels of COL6A2 evaluated respectively by real-time PCR and immunoblotting in MDA-MB-231 cells exposed to vehicle (–) or 50 ng/ml IGF1, as indicated. **C** COL6A2 levels evaluated by ELISA in the supernatants collected from MDA-MB-231 exposed to vehicle (–) or 50 ng/ml IGF1. **D** Protein levels of COL6A2 in MDA-MB-231 cells exposed for 1 h to vehicle (–) or 50 ng/ml IGF1 alone or in combination with 1 µM IGF1R inhibitor OSI-906. **E** Correlation analysis of IGF1 and COL6A2 in TNBC patients of the TCGA cohort. The Pearson correlation coefficient (r) and the relative p-value are shown in the panel. **F** Immunoprecipitation assays performed in MDA-MB-231 cells exposed to vehicle (–) or 50 ng/ml IGF1 alone or in combination with 1 µM IGF1R inhibitor OSI-906. Cell lysates were immunoprecipitated with an anti-DDR1 antibody and DDR1 phosphorylation was assessed using a phosphotyrosine antibody (p-Tyr). In control samples, nonspecific IgG was used instead of the primary antibody. An equal amount of the total lysates (input) was blotted for DDR1 as loading control. **G** MDA-MB-231 cells were transiently transfected with a constitutive empty vector (EV) or the mutant K618A DDR1 (DDR1/K618A) expressing plasmid. After 48 h, cells were exposed to vehicle (–) or 50 ng/ml IGF1 for 1 h, lysed and subjected to immunoprecipitation and immunoblotting assays to detect DDR1 phosphorylation levels, as described above. **H** Correlation between the mRNA expression levels of COL6A2 and IL1-β in TNBC patients of the TCGA dataset, as ascertained by calculating the Pearson correlation coefficient (r). p-value is indicated in the panel. (I) Kaplan–Meier curve showing the correlation of high cumulative expression of COL6A2 and IL1-β with worse disease-free interval (DFI) in TNBC patients of TCGA. p-value is indicated in the panel. mRNA (**J**) and protein (**K**) levels of IL1-β evaluated respectively by real-time PCR and immunoblotting in MDA-MB-231 cells exposed to vehicle (–) or 50 ng/ml IGF1, as indicated. **L** IL1-β levels evaluated by ELISA in the supernatants deriving from MDA-MB-231 cells exposed to vehicle (–) or 50 ng/ml IGF1. In RNA experiments, values are normalized to the actin beta (ACTB) expression and presented as fold changes of mRNA expression upon treatments relative to the vehicle. Side panels show densitometric analysis of the blots normalized to the loading control. Results shown are representative of at least three independent experiments. (*) indicates $p < 0.05$

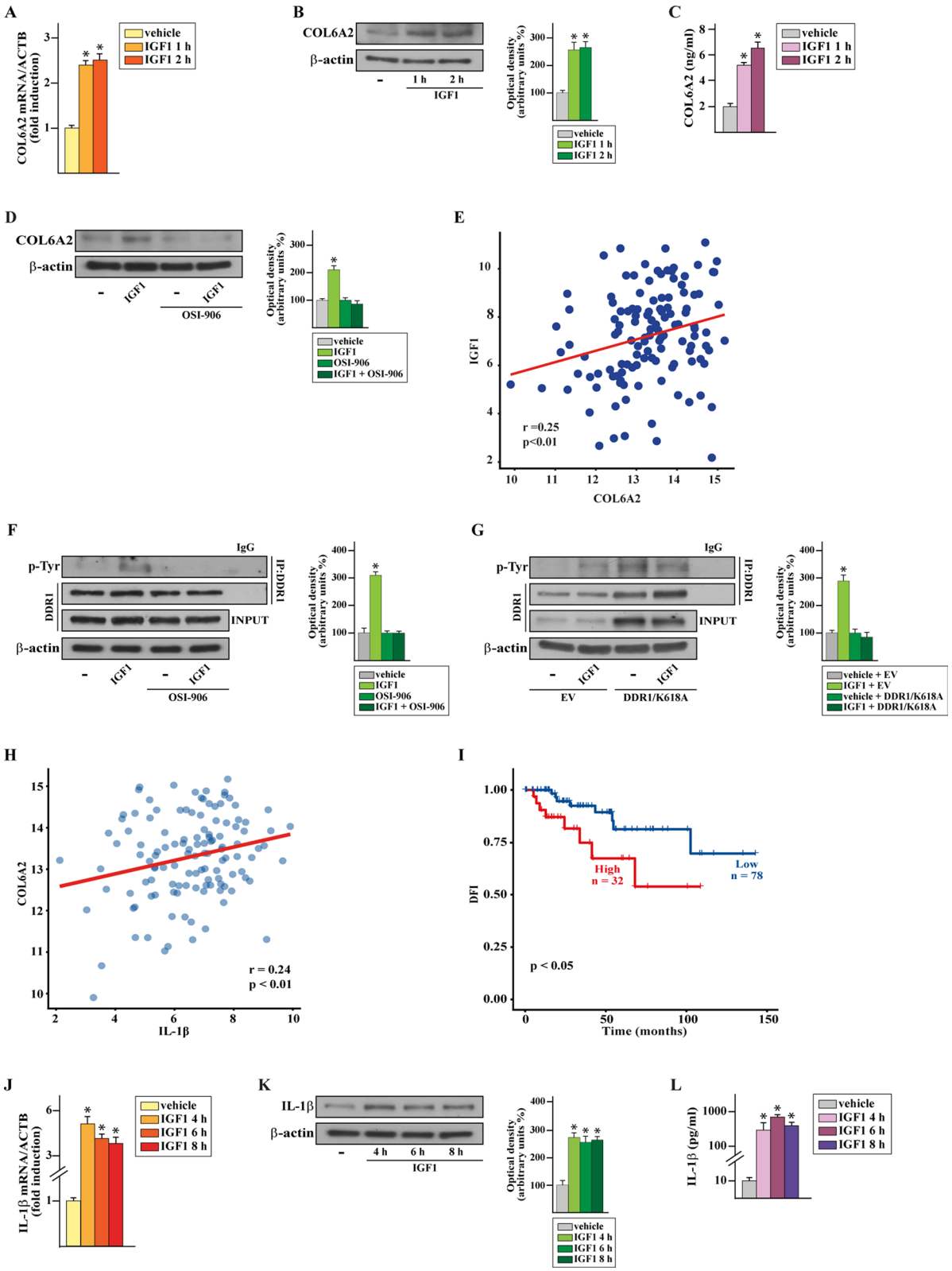

Fig. 1 (See legend on previous page.)

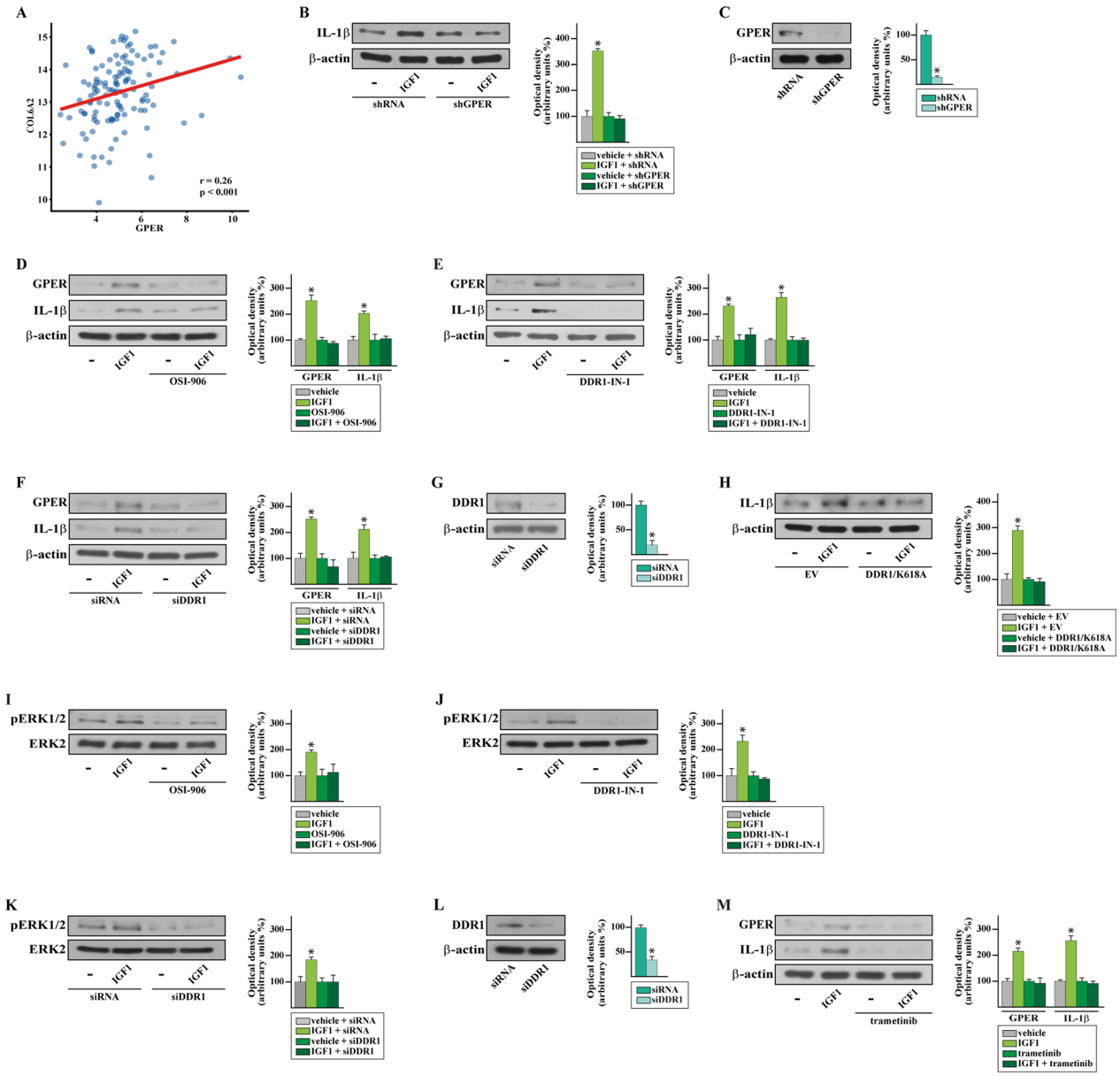

Fig. 2 The DDR1/ERK/GPER signaling is involved in the induction of IL1-β by IGF1 in TNBC cells. **A** Scatter plot depicting the correlation between COL6A2 and GPER gene expression in TNBC patients of the TCGA dataset, the Pearson correlation coefficient (r) and the relative p-value are indicated within the panel. **B** Immunoblot of IL1-β from GPER-silenced MDA-MB-231 cells exposed to vehicle (–) or 50 ng/ml IGF1. **C** Efficacy of GPER silencing in MDA-MB-231 cells. Protein levels of GPER and IL1-β in MDA-MB-231 cells exposed for 4 h to vehicle or 50 ng/ml IGF1 alone or in combination with 1 μM IGF1R inhibitor OSI-906 (**D**) or DDR1 inhibitor DDR1-IN-1 (**E**). **F** Immunoblots of GPER and IL1-β from DDR1-silenced MDA-MB-231 cells exposed to vehicle (–) or 50 ng/ml IGF1. **G** Efficacy of DDR1 silencing in MDA-MB-231 cells. **H** Protein levels of IL1-β in MDA-MB-231 cells transiently transfected with a constitutive empty vector (EV) or the mutant K618A DDR1 (DDR1/K618A) expressing plasmid, and thereafter exposed to vehicle (–) or 50 ng/ml IGF1 for 4 h. ERK1/2 phosphorylation in MDA-MB-231 cells treated for 1 h with vehicle (–) or 50 ng/ml IGF1 in the presence of 1 μM IGF1R inhibitor OSI-906 (**I**) or 1 μM DDR1 inhibitor DDR1-IN-1 (**J**) or in MDA-MB-231 cells transiently transfected with scramble siRNA or siRNA targeting DDR1 (**K**). **L** Efficacy of DDR1 silencing in MDA-MB-231 cells. **M** Immunoblots of GPER and IL1-β in MDA-MB-231 cells exposed for 4 h to vehicle or 50 ng/ml IGF1 in the presence or absence of 100 nM trametinib. Side panels show densitometric analyses of the blots normalized to β-actin or ERK2 that served as loading controls, as indicated. Values represent the mean ± SD of three independent experiments performed in triplicate. (*) indicates $p < 0.05$

ELISA Kit (MyBioSource, SIAL, Rome, Italy) and human IL-1β ELISA Kit (Thermo Scientific, Monza, Italy), respectively, according to the manufacturer's instructions. The plates were read at 450 nm on a Microplate Spectrophotometer Epoch™ (BioTek, AHSI, Milan Italy).

Conditioned medium

MDA-MB-231 cells were cultured in the regular growth medium, switched to medium without serum for 24 h and then treated with vehicle or 50 ng/ml IGF1 for 4 h. Thereafter, cells were washed and placed in fresh medium containing 5% charcoal-stripped FBS for additional 18 h. The supernatants were collected, centrifuged at 3500 rpm for 5 min to remove cell debris and used as conditioned medium in the appropriate experiments.

Proliferation assay

Cells (1×10^4) were seeded in 24-well plates in regular growth medium and once attached they were washed and incubated in a medium containing 2.5% charcoal-stripped FBS and then exposed to treatments, as indicated. Transfections were renewed every 2 days, when required, and treatments every day. The proliferation rate was calculated by counting the cells on day 5 using the Countess Automated Cell Counter, as recommended by the manufacturer's protocol (Thermo Fisher Scientific, Milan, Italy).

Spheroid formation assay

Spheroids were generated by dispensing 100 µL of a single-cell suspension (1×10^4 cells/well) into 96-well plates pre-coated with 2% agarose to prevent cell attachment and promote three-dimensional aggregation. Three days after seeding, 50% of the culture medium was replaced with fresh medium containing the appropriate treatment conditions. This partial medium change was repeated every 2 days. When required, transfections were also renewed every 2 days, following the same schedule as medium replenishment. On day 8, spheroids were imaged using the Cytation 3 Cell Imaging Multimode Reader (BioTek, AHSI, Milan, Italy). Spheroid area was quantified using Gen5 software (BioTek, AHSI, Milan, Italy), which enables automated image analysis.

Spheroid culture in rotating bioreactors

Bioreactor cultures were generated according to the manufacturer's instructions. Briefly, 2 ml of 1% sodium alginate solution, in which 1×10^3/µl cells were suspended, was inserted in the bioreactors (clinoReactors, CelVivo ApS, Odense, Denmark). 60 drops of sodium alginate beads encapsulating cells/reactor were dotted into a crosslinking solution, which was previously added to the clinoReactors. After polymerization, the crosslinking solution was removed and spheroids were submerged in the appropriate medium. Bioreactors were subsequently placed into the ClinoStar system (CelVivo ApS) and spheroids were cultivated at 37 °C, 5% CO2 and 95% air for 10 days with continuous rotation of the bioreactors. Spheroids were then collected and transferred into 24-well tissue culture plates, and imaged using the ImageFocus Plus V2 software of the inverted Oxion Inverso microscope (Euromex).

MTT assay for cell viability

The proliferation rate of MDA-MB-231 cells cultured within sodium alginate beads in the stirred bioreactors was assessed by MTT assay (Merck, Milan, Italy), as described elsewhere [45]. Briefly, after 21 days, the cells were released from the beads by using a solution containing 200 mM sodium bicarbonate and 60 mM sodium citrate. Cells were collected by centrifugation at 1000 rpm for 5 min, and 1 ml MTT solution (5 mg/10 mL of medium) was then added before incubating the cells at 37 °C in a humidified atmosphere (95% air and 5% CO2) for 4 h. Afterward, the MTT solution was removed and replaced with 500 µL dimethyl sulfoxide (DMSO). Finally, the absorbance of the samples was measured at 570 nm using a Microplate Spectrophotometer Epoch™ (BioTek, AHSI, Milan Italy). The absorbance values were normalized by the number of beads per sample.

(See figure on next page.)

Fig. 3 The IGF1R/DDR1/GPER/ERK-dependent increase of c-fos mediates the up-regulation of IL1-β in TNBC cells. Immunoblots of c-fos in MDA-MB-231 cells exposed for 4 h to vehicle (–) or 50 ng/ml IGF1 in the presence of 1 µM IGF1R inhibitor OSI-906 (**A**) or DDR1 inhibitor DDR1-IN-1 (**B**). c-Fos protein levels in DDR1 (**C**) and GPER-silenced (**E**) MDA-MB-231 cells. Efficacy of DDR1 (**D**) and GPER (**F**) silencing in MDA-MB-231 cells. **G** Immunoblot of c-fos in MDA-MB-231 cells exposed for 4 h to vehicle or 50 ng/ml IGF1 in the presence or absence of 100 nM trametinib. **H** IL-1β protein levels in MDA-MB-231 cells transfected with a scramble or a dominant-negative c-fos construct (DN/c-fos) and thereafter exposed for 4 h to vehicle (–) or 50 ng/ml IGF1. Side panels show densitometric analyses of the blots normalized to β-actin that served as loading control. **I** Recruitment of c-fos to the AP-1 site located within the IL1-β promoter, as ascertained by ChIP assay in MDA-MB-231 cells exposed for 4 h to vehicle or 50 ng/ml IGF1. In control samples, nonspecific IgG were used instead of the primary antibody. The amplified sequences were evaluated by real-time PCR. Values represent the mean ± SD of three independent experiments performed in triplicate. (*) indicates $p < 0.05$

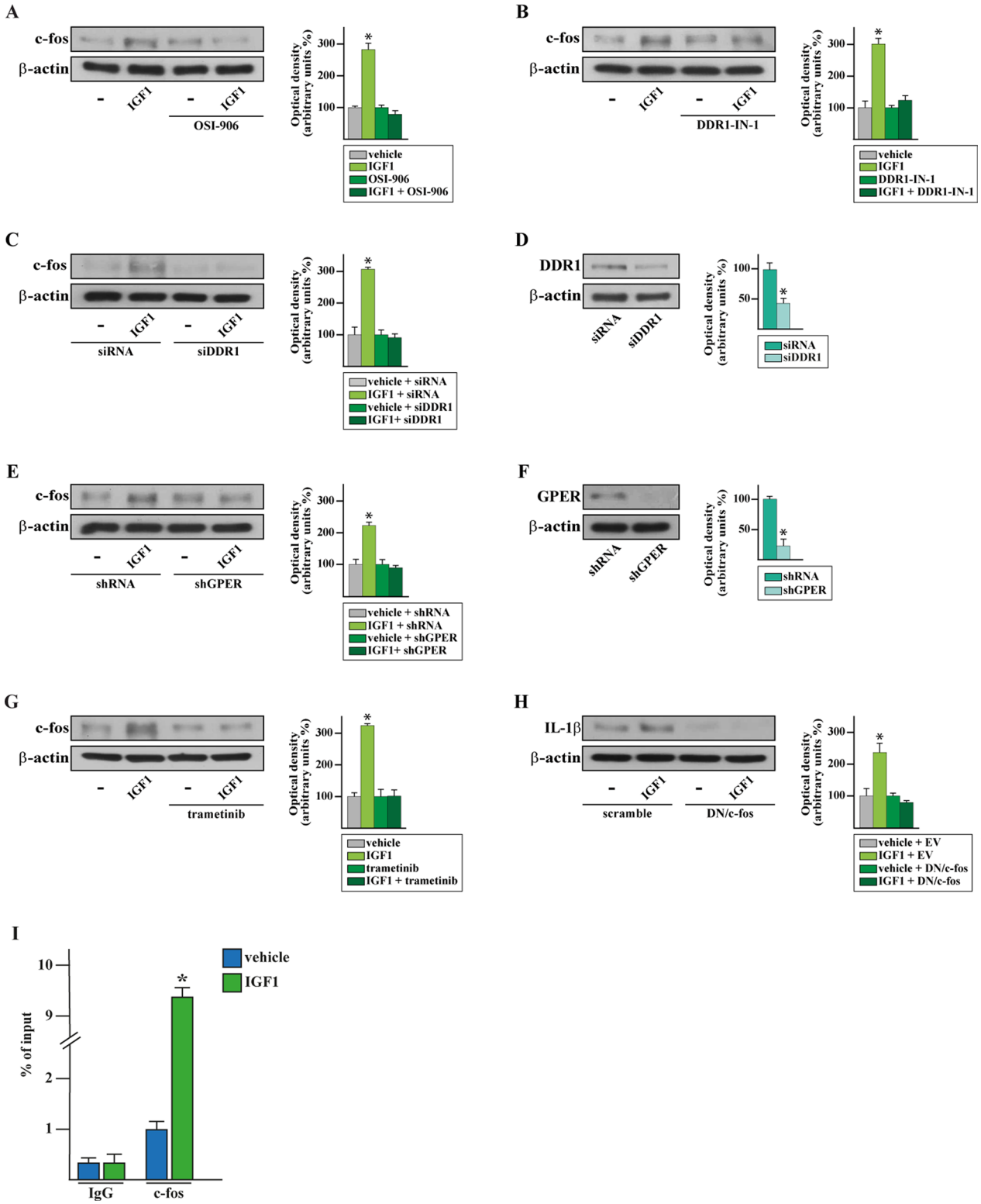

Fig. 3 (See legend on previous page.)

Migration assay

Transwell 8 µm polycarbonate membranes (Costar, Merck, Milan, Italy) were used to evaluate cell migration. In 300 µl serum free medium, MDA-MB-231 cells (3×10^4) were seeded in the upper chamber and co-cultured with WI38 cells previously exposed to treatments in the bottom chamber. 8 h after co-culturing, cells on the upper surface of the membrane were then removed by wiping with Q-tip, and migrated cells were fixed with 100% methanol, stained with Giemsa (Merck, Milan, Italy), photographed using a digital camera and counted using the WCIF ImageJ software.

Matrigel drops evasion assay

The matrigel drop assay was performed as previously described [46]. Briefly, 5×10^4/drop of MDA-MB-231 and MDA-MB-436 cells, previously transfected when needed, were suspended in 10 µl of Corning Matrigel Growth Factor Reduced (GFR) Basement Membrane Matrix (Merck, Milan, Italy). The cell/matrigel suspension was layered onto the surface of a 12-well plate to form a well-defined drop and placed at 37 °C to solidify. Medium containing 5% charcoal-stripped FBS and treatments were placed over the drop. Cells were observed at specified time points and drops were photographed using the ImageFocus Plus V2 software of the inverted Oxion Inverso microscope (Euromex). The number of cells migrated out of the drop was measured.

Statistical analysis

Statistical analyses were performed using ANOVA followed by Newman-Keuls' test to determine differences in means. Scatter plots were drawn with the R tidyverse package.

Results

The IGF1/IGF1R axis triggers both the activation of DDR1 induced by collagen VI and the up-regulation of IL-1β in TNBC cells

Previous studies suggested that IGF1 promotes collagen synthesis in diverse physio-pathological contexts [47, 48]. On these bases and considering that both IGF1 and collagen play an important role in regulating BC growth and therapy resistance [15, 49–53], we aimed to investigate whether a pro-tumorigenic relationship between IGF1 and collagen may occur in TNBC cells. In particular, we focused our attention on the potential of IGF1 to regulate collagen VI, which is a fat-related collagen type fueling BC progression [54–57]. First, we found that IGF1 rapidly increases the expression and secretion of the alpha-2 subunit of collagen VI (COL6A2) in MDA-MB-231 (Fig. 1A-C) and MDA-MB-436 (Additional file 1) TNBC cells. As expected, the IGF1R inhibitor OSI-906 prevented the IGF1-induced protein increase of COL6A2 in MDA-MB-231 cells (Fig. 1D). Nicely fitting with these results, a positive correlation between IGF1 and COL6A2 gene expression levels was found in TNBC patients of the TCGA database (Fig. 1E). Considering that collagens are the only known ligands for the discoidin domain receptor 1 (DDR1) and a functional crosstalk between IGF1R and DDR1 promotes BC progression [43, 58, 59], we next aimed at exploring whether the IGF1/IGF1R signaling could engage DDR1 activation via COL6A2 in TNBC cells. In accordance with our previous studies [43], IGF1 demonstrated the ability to stimulate the phosphorylation of DDR1 in an IGF1R-dependent manner, as observed using OSI-906 (Fig. 1F). To determine whether the IGF1-induced DDR1 activation relies on COL6A2, we assessed that the DDR1 phosphorylation is no longer detectable in TNBC cells overexpressing a kinase-inactive DDR1/K618A mutant (Fig. 1G), which fails to respond to collagen stimulation. Together, these results

(See figure on next page.)

Fig. 4 The IL1-β/IL1R1 signaling is implicated in the IGF1-induced growth of TNBC cells. **A** Proliferation of MDA-MB-231 cells after 5 days treatment with vehicle or 50 ng/ml IGF1 alone or in combination with 1 µM IGF1R inhibitor OSI-906 or DDR1 inhibitor DDR1-IN-1, as indicated. (**B**) Growth assays in MDA-MB-231 cells transfected every 2 days with shRNA or shGPER, treated every day with vehicle or 50 ng/ml IGF1 and then counted after 5 days. **C** Proliferation of MDA-MB-231 cells after 5 days treatment with vehicle or 50 ng/ml IGF1 alone or in combination with 5 µg/ml IL-1R1 antagonist raleukin. Values of vehicle-treated cells were set as 100% upon which cell viability was determined. **D** Representative pictures of spheroids (a single spheroid/well) from the MDA-MB-231 spheroid cultures grown on agar-coated plates and exposed for 8 days to vehicle or 50 ng/ml IGF1 alone or in combination with 1 µM IGF1R inhibitor OSI-906 or 1 µM DDR1 inhibitor DDR1-IN-1. (F) Representative pictures of spheroids (a single spheroid/well) from GPER-silenced MDA-MB-231 cells grown for 8 days on agar-coated plates. Spheroids were transfected every 2 days with shRNA or shGPER, treated every 2 days and then counted on day 6. Scale bar: 1000 µm. (H) Efficacy of GPER silencing in MDA-MB-231 cells. The bottom panel shows densitometric analyses of the blots normalized to β-actin that served as loading control. **I** Representative pictures of spheroids (a single spheroid/well) from the MDA-MB-231 spheroid cultures grown on agar-coated plates and exposed for 8 days to vehicle or 50 ng/ml IGF1 alone or in combination with 5 µg/ml IL-1R1 antagonist raleukin. **E**, **G**, **J** Quantification of spheroid growth. Values of vehicle-treated MDA-MB-231 cells were set as 100% upon which spheroid growth was determined. Values represent the mean ± SD of three independent experiments performed in triplicate. (*) indicates $p < 0.05$

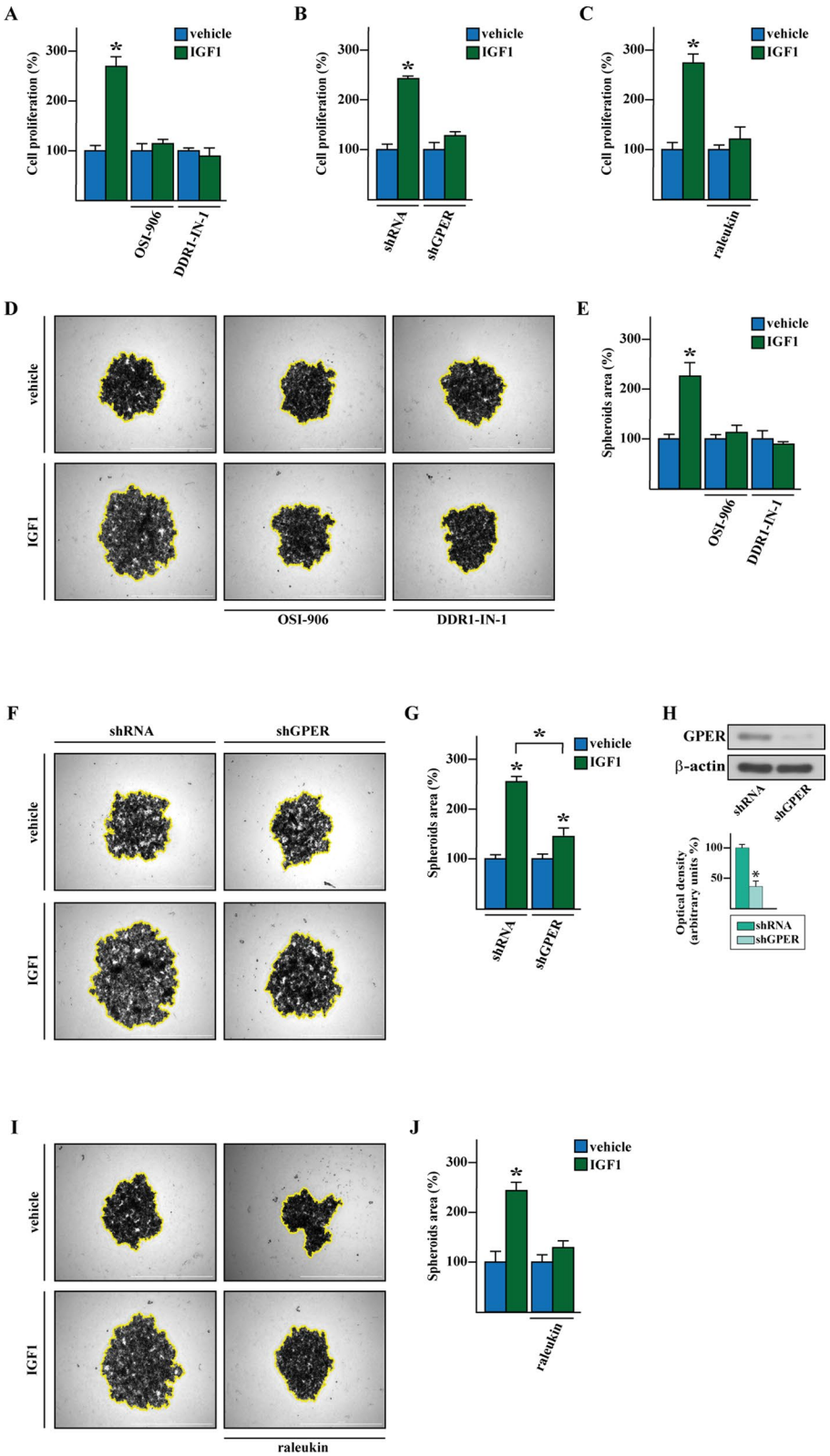

Fig. 4 (See legend on previous page.)

point to a collagen VI-dependent mechanism by which the IGF1/IGF1R axis activates DDR1 in TNBC cells.

Previous findings have revealed that collagen up-regulation in TNBC cells may enhance chemoresistance by stimulating cytokine-mediated transduction pathways [49]. This prompted us to investigate whether COL6A2 can regulate the expression of a main mediator of inflammation-driven breast carcinogenesis, like IL-1β [34, 60–62]. In this regard, we assessed that a positive correlation between the levels of COL6A2 and IL-1β occurs in TNBC patients of the TCGA dataset (Fig. 1H). In order to evaluate the clinical significance of these genes, we performed survival analyses. Notably, we found that a high cumulative expression of COL6A2 and IL-1β is associated with poor outcomes in terms of disease-free interval (DFI) in TNBC patients (Fig. 1I). Accordingly, we ascertained that IGFI induces the mRNA and protein expression as well as the secretion of IL-1β in MDA-MB-231 (Fig. 1J-L) and MDA-MB-436 (Additional File 1) cells.

The IGF1/IGF1R axis stimulates IL-1β expression through the DDR1/ERK/GPER signaling pathway in TNBC cells

Our previous data suggested the involvement of the membrane estrogen receptor named GPER in the regulation of IL-1β in BC cells as well as in the functional cooperation with both IGF1R and DDR1 toward collagen increase [18, 21, 23, 34]. Reminiscing these data, we determined the role of GPER in the collagen VI-mediated activation of DDR1 as well as in the increase of IL-1β in TNBC cells upon IGF1 exposure. First, we discovered a positive correlation between COL6A2 and GPER expression levels occurring TNBC in patients (Fig. 2A). Then, we demonstrated that the up-regulation of IL-1β by IGF1 is abolished by silencing GPER expression (Fig. 2B-C). In addition, we ascertained that the induction of both GPER and IL-1β by IGF1 is abrogated by OSI-906 (Fig. 2D) as well as using the DDR1 inhibitor named DDR1-IN-1 (Fig. 2E) or knocking down DDR1 by using a specific siRNA (Fig. 2F-G). We also determined that IGF1 lacks the ability to induce IL-1β in cells expressing the DDR1/K618A mutant (Fig. 2H), further suggesting that DDR1 phosphorylation by collagen VI is required for the up-regulation of both GPER and IL-1β in TNBC cells upon activation of the IGF1/IGF1R signaling.

In order to provide novel insights on the transduction mechanisms regulating IL-1β expression by IGF1, we focused on the ERK1/2 cascade based on previous studies indicating that DDR1 activation by collagen triggers the ERK signaling pathway in cancer cells [63]. In this vein, we ascertained that the activation of ERK1/2 is prevented using OSI-906 (Fig. 2I) as well as inhibiting (Fig. 2J) or silencing DDR1 (Fig. 2K, L). Nicely fitting with these results, the MEK inhibitor trametinib prevented the protein induction of both GPER and IL-1β observed upon IGF1 treatment (Fig. 2M). Next, we aimed to explore the role of the main molecular sensor of GPER signaling, namely c-fos, in the up-regulation of IL-1β prompted by IGF1. Of note, the increased c-fos levels upon IGF1 exposure were no longer present using OSI-906 (Fig. 3A) and DDR1-IN-1 (Fig. 3B) as well as silencing DDR1 (Fig. 3C, D) or GPER (Fig. 3E, F). In line with previous studies demonstrating that the ERK1/2 signaling pathway regulates the expression of c-fos [18, 64], which in turn has been implicated in the regulation of IL-1β [34], we established that trametinib prevents the protein increase of c-fos triggered by IGF1 (Fig. 3G). Accordingly, the plasmid encoding a dominant negative c-fos (DN/c-fos) abrogated the up-regulation of IL-1β observed upon IGF1 exposure (Fig. 3H), and ChIP assays revealed that IGF1 induces the binding of c-fos to an AP-1 site located within the IL-1β promoter sequence (Fig. 3I). Collectively, these findings suggest that the IGF1/IGF1R system triggers the collagen-mediated DDR1/ERK activation toward the induction of the GPER/c-fos/IL-1β transduction pathway in TNBC cells.

IL-1β/IL1R1 transduction signaling contributes to the proliferation and motility of TNBC cells induced by IGF1 through the activation of the IGF1R/DDR1/GPER axis

On the basis of the above data, we sought to provide insights into the biological responses promoted by IGF1 in TNBC cells through IL-1β. In both MDA-MB-231

(See figure on next page.)

Fig. 5 IGF1 promotes the motile behavior of TNBC cells by engaging the IL1-β/IL1R1 axis. **A** Representative pictures from the matrigel drops evasion assays in MDA-MB-231 cells treated with vehicle or 50 ng/ml IGF1 alone or in combination with 1 μM IR inhibitor OSI-906 or DDR1 inhibitor DDR1-IN-1, as indicated. **C** Representative pictures from the matrigel drops evasion assays in GPER-silenced MDA-MB-231 cells treated vehicle or 50 ng/ml IGF1. **E** Efficacy of GPER silencing in MDA-MB-231 cells. Side panel shows densitometric analyses of the blots normalized to β-actin that served as loading control. **F** Representative pictures from the matrigel drops evasion assay in MDA-MB-231 cells treated with vehicle or 50 ng/ml IGF1 alone or in combination with or 5 μg/ml IL-1R1 antagonist raleukin. **B**, **D**, **G** Percentage of cells around the drop upon 3 days treatment from three independent experiments performed in triplicate. Values of vehicle-treated MDA-MB-231 cells were set as 100% upon which evading cell percentage was determined. Dotted line indicates the matrigel drop border. Scale bar: 200 μm. (*) indicates $p < 0.05$

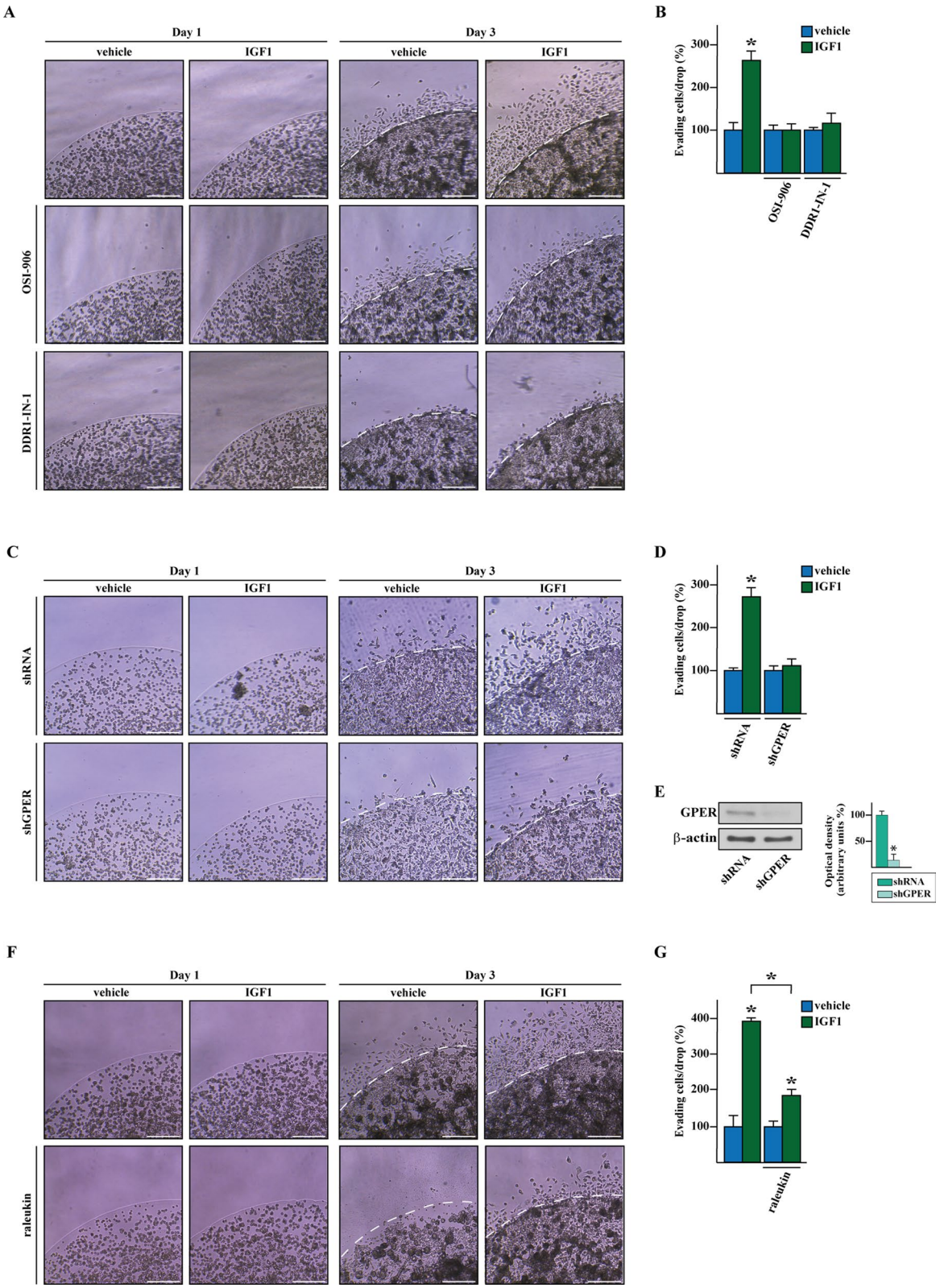

Fig. 5 (See legend on previous page.)

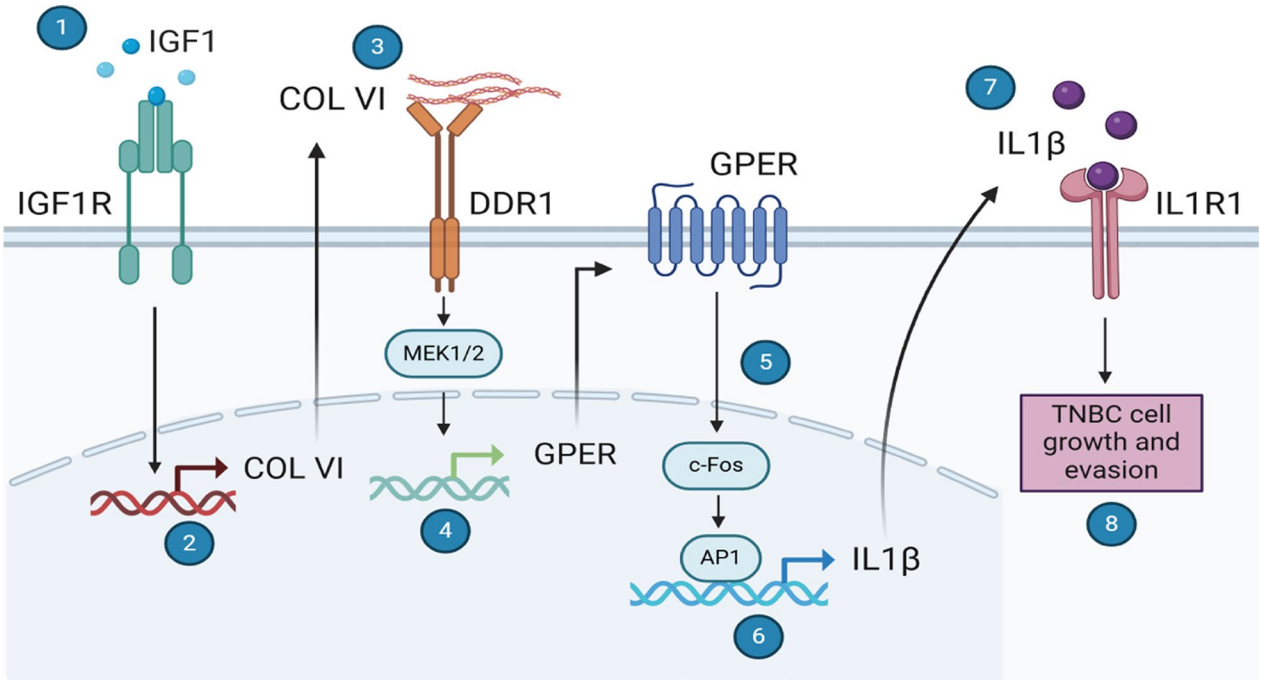

Fig. 6 Schematic showing model whereby IGF1/IGF1R signaling induces collagen VI-dependent DDR1 activation, ERK-mediated GPER and c-fos increase toward the up-regulation of IL-1β. IL-1β/IL1R1 signaling, in turn, contributes to proliferative and motile characteristics in TNBC cells through an autocrine mechanism. Created in https://BioRender.com

(See figure on next page.)

Fig. 7 IL-1β stimulates the reprogramming of normal fibroblasts into CAFs-like cells that in turn stimulate aggressive features in TNBC cells. **A** FAP expression evaluated by immunofluorescence assays in WI38 cells cultured for 72 h with conditioned medium (CM) collected from MDA-MB-231 cells previously exposed for 4 h to vehicle or 50 ng/ml IGF1 alone or in combination with 5 μg/ml IL-1R1 antagonist raleukin. Nuclei were stained by DAPI. Scale bar: 100 μm. **C** Representative pictures of spheroids (a single spheroid/well) grown for 6 days on agar-coated plates from WI38 cells cultured for 72 h with conditioned medium (CM) collected from MDA-MB-231 cells previously exposed for 4 h to vehicle or 50 ng/ml IGF1 alone or in combination with 5 μg/ml IL-1R1 antagonist raleukin. Scale bar: 1000 μm. **E** FAP expression evaluated by immunofluorescence assays in WI38 cells exposed to vehicle or IL-1β (10 ng/ml) alone or in combination with 5 μg/ml IL-1R1 antagonist raleukin. Nuclei were stained by DAPI. Scale bar: 100 μm. **B**, **F** Fluorescence intensities were quantified in 20 random fields for each condition and results are expressed as fold change of relative fluorescence units (RFU) over vehicle-treated cells (set as one-fold induction). **G** Representative pictures of spheroids (a single spheroid/well) grown for 6 days on agar-coated plates from WI38 cells exposed for 72 h to vehicle or IL-1β (10 ng/ml) alone or in combination with 5 μg/ml IL-1R1 antagonist raleukin. Scale bar: 1000 μm. **D**, **H** Quantification of spheroid growth. Values of vehicle-treated WI38 cells were set as 100% upon which spheroid growth was determined. **I** Transwell migration assays in MDA-MB-231 cells co-cultured for 8 h with WI38 cells (NFs) cultured for 72 h with conditioned medium (CM) collected from MDA-MB-231 cells, which were previously exposed for 4 h to vehicle or 50 ng/ml IGF1 alone or in combination with 5 μg/ml IL-1R1 antagonist raleukin. **K** Representative pictures of sodium alginate beads encapsulating MDA-MB-231 cells cultured for 10 days in bioreactors in the presence of the conditioned medium (CM) of WI38 cells (NFs) treated for 72 h with the conditioned medium (CM) collected from MDA-MB-231 cells, which were previously exposed for 4 h to vehicle or 50 ng/ml IGF1, alone or in combination with 5 μg/ml IL-1R1 antagonist raleukin. **M** Transwell migration assay in MDA-MB-231 cells co-cultured for 8 h with WI38 cells (NFs) previously exposed for 72 h to vehicle (–) or IL-1β (10 ng/ml) alone or in combination with 5 μg/ml IL-1R1 antagonist raleukin. **J**, **N** Cells were counted in at least 5 random fields in three independent experiments performed in triplicate. Scale bar: 100 μm. **O** Representative pictures of sodium alginate beads encapsulating MDA-MB-231 cells cultured for 10 days in bioreactors with the conditioned medium (CM) of WI38 cells (NFs) exposed for 72 h to vehicle (–) or IL-1β (10 ng/ml) alone or in combination with 5 μg/ml IL-1R1 antagonist raleukin. (L, P) Cell viability of MDA-MB-231 in the sodium alginate beads. Scale bar: 1000 μm. Values of vehicle-treated MDA-MB-231 cells were set as 100% upon which cell viability was determined. Data shown are the mean ± SD of three independent experiments performed in triplicate. (*) indicates $p < 0.05$. **Q** Cartoon depicting the molecular events and the biological responses triggered by IL-1β within the TNBC microenvironment. Created with BioRender.com

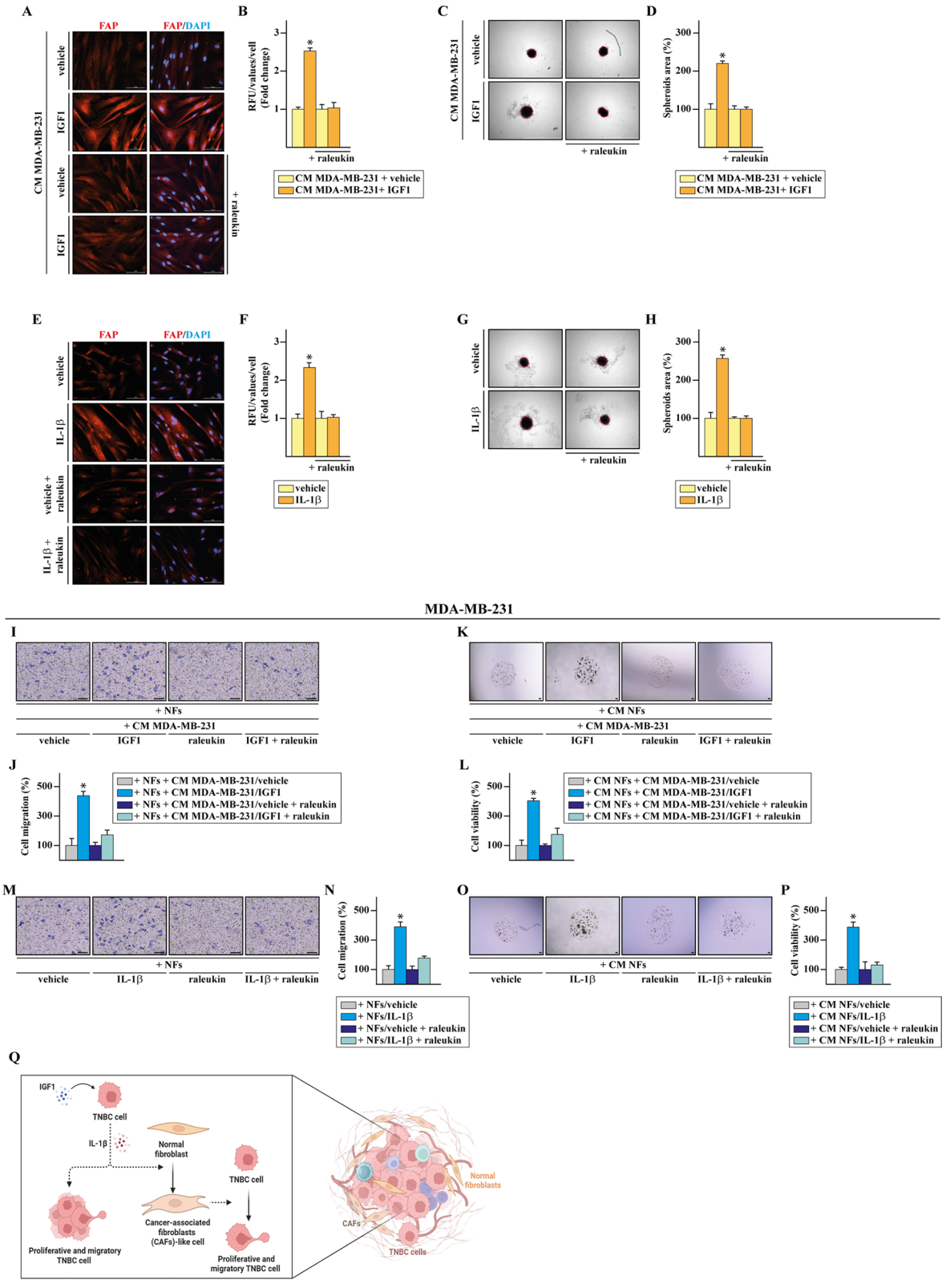

Fig. 7 (See legend on previous page.)

and MDA-MB-436 cells, the inhibition of IGF1R or DDR1 (Fig. 4A,D, E; Additional file 2) as well as the depletion of GPER levels (Fig. 4B,F–H; Additional file 2) resulted in the reduction of IGF1-stimulated growth in two-dimensional (2D) and three-dimensional (3D) culture models. These effects were no longer evident also using the IL1R1 antagonist raleukin (Fig. 4C, I, J; Additional file 2), suggesting the involvement of IL-1β and the activation of its cognate receptor in the proliferative responses triggered by IGF1 in TNBC cells. Results similar to those described above were obtained in 3D matrigel drops evasion assays (Fig. 5; Additional file 3), indicating that IGF1R, DDR1, GPER and the IL-1β/IL1R axis contribute to the enhanced motility of TNBC cells upon IGF1 exposure (Fig. 6).

IL-1β induces the reprogramming of normal fibroblasts into CAFs-like cells toward tumor-supporting events in TNBC cells

Within the TME, CAFs constitute a population of heterogeneous cellular components that reflect, in terms of phenotypic features, the diverse cells they originate from [65]. In particular, normal fibroblasts can be recruited within the TME, activated and reprogrammed into CAFs in response to chemokines, cytokines, and growth factors released by cancer cells and stromal components [66]. In view of these observations and previous evidence indicating that CAFs exhibit an increased expression of certain markers, such as the fibroblast activation protein (FAP), and greater proliferation and migration properties than normal fibroblasts [67, 68], we hypothesized that the secretion of IL-1β induced by IGF may stimulate normal fibroblasts to acquire a CAFs-like phenotype. Hence, we maintained normal fibroblasts in medium from MDA-MB-231 cells previously exposed to IGF1. After 72 h, the fibroblasts expressed higher protein levels of a distinctive CAFs marker named FAP (Fig. 7A-B). In addition, a higher proliferative ability of normal fibroblasts exposed to culture media derived from IGF1-treated MDA-MB-231 cells was observed (Fig. 7C-D). Of note, raleukin lessened both the up-regulation of FAP (Fig. 7A-B) and the biological properties (Fig. 7C-D) acquired by the fibroblasts. Results similar to those described above were observed treating cells with the recombinant human IL-1β (Fig. 7E-H).

To examine the potential influence of IL-1β-activated fibroblasts on TNBC cells, we co-cultured MDA-MB-231 cells with normal fibroblasts previously incubated with the CM deriving from IGF1-treated MDA-MB-231 cells. Of note, the CM from CAFs-like cells promoted TNBC cell migration (Fig. 7I-J). Turning to a 3D bioreactor platform in order to mimic the in vivo environment, we observed that the CM derived from CAFs-like cells stimulates proliferative effects in MDA-MB-231 cells encapsulated in sodium alginate beads (Fig. 7K, L). These data were further confirmed by directly exposing normal fibroblasts to IL-1β in the presence or absence of raleukin (Fig. 7M, P). Therefore, the acquisition of CAFs-like features by normal fibroblasts triggers aggressive properties in TNBC cells in the context of a feed-forward stimulation occurring between cancer cells and the surrounding stroma. Altogether, our findings suggest that the IL-1β production by TNBC cells exposed to IGF1 treatment may promote the acquisition of a CAFs-like phenotype by normal fibroblasts toward their tumor-supportive role within the TNBC microenvironment (Fig. 7Q).

Discussion

Tumor-promoting inflammation fosters multiple hallmark capabilities of cancer [69]. It can supply a variety of bioactive molecules that stimulate proliferative, survival, angiogenic, invasive and metastatic responses within the TME [70]. In this context, the low-grade inflammatory state associated with obesity has been strictly linked to the pathophysiology of diverse obesity-related diseases, including cancer [71–73]. Among other types of tumors, obesity has been correlated with a high prevalence of TNBC, serving also as a potential predictor of sensitivity to neoadjuvant chemotherapy in patients affected by this aggressive malignancy [74]. Multiple local and systemic events may contribute to the association of obesity with cancer, including elevated circulating insulin and glucose levels, IGF1 bioavailability, as well as adipose-derived cytokines, hormones and growth factors, referred to as adipokines [75]. Additionally, the adipose tissue of obese individuals is the main site of innate immune cells, which in turn generate pro-inflammatory molecules further promoting tumor aggressiveness [71, 74, 76]. In particular, IL-1β has emerged as a crucial modulator of tumor-promoting inflammatory responses due to its ability to target diverse TME components toward the suppression of anti-tumor immunity events along with the promotion of angiogenesis and invasive features [77, 78]. Of note, clinical studies have also demonstrated that high circulating levels of IL-1β are linked to worse outcomes in patients with diverse cancer types [79]. As it concerns BC, primary tumors characterized by an elevated IL-1β expression do exhibit a higher chance of developing metastatic disease [80].

On the basis of these findings and previous data indicating that the IGF system is implicated in BC progression, particularly during obesity [11, 13, 52], we aimed to provide novel insights into the molecular regulation and biological function of IL-1β in TNBC cells upon IGF-1 exposure. Remarkably, our findings demonstrate that the IGF1/IGF1R axis triggers the activation of DDR1 and

the subsequent up-regulation of GPER along with one of its main target genes namely c-fos, leading to increased expression and secretion of IL-1β in TNBC cells. In turn, the IL-1β/IL1R1 signaling promoted TNBC cell expansion and invasion in an autocrine manner. These data are consistent with our previous studies showing that the alternate estrogen receptor GPER is involved in the activation of IL-1β/IL1R1 signaling and invasive features triggered by a further hallmark of cancer, namely hypoxia, in both TNBC cells and CAFs [34]. Moreover, we have previously found that GPER contributes to the functional cooperation between IGF1R and DDR1 [17, 18, 23, 34]. In particular, the IGF1/IGF1R transduction pathway has been engaged in the activation of both GPER and DDR1 toward the transcription of their target genes, which in turn stimulate a feedforward loop leading to the up-regulation of GPER, DDR1 and IGF-1R levels [23, 43]. The crosstalk among these factors is implicated in the potentiation of mitogenic responses elicited by IGF1 in BC cells [23]. In the present study, we have provided novel findings demonstrating that the IGF1-dependent release of a major extracellular matrix protein, named collagen VI, is involved in the up-regulation of IL-1β in TNBC cells. In line with previous data indicating that collagen VI increases in the stroma of obese TNBC patients and drives the invasion of TNBC cells [56], here we establish for the first time that the increase of collagen VI upon IGF1 exposure is required for the activation of DDR1 toward the IL-1β-mediated aggressive features of TNBC cells.

In addition, the present investigation highlighted the tumor-supporting molecular events engaged by IL-1β within the TME. Notably, we ascertained that this cytokine contributes to reprogramming normal fibroblasts into CAFs-like cells. In this regard, we assessed that the conditioned medium from IGF1-treated TNBC cells induces the expression of CAFs-related markers in normal fibroblasts that gain strengthened proliferative capabilities. To date, one key challenge in depicting the role of the TME, with significant implications for the development of novel therapeutic strategies, stands for the high heterogeneity of CAFs that is consequent to their various origins. Indeed, CAFs can derive from different cell types like stellate cells, smooth muscle cells, endothelial cells, adipocytes, mesenchymal stem cells, pericytes, epithelial cells as well as normal fibroblasts [65, 81]. In particular, it has been shown that breast cancer cells trigger multiple paracrine signals that facilitate the transition of normal fibroblasts into CAFs to provide a supportive TME [82–84]. During the initial stages of the carcinogenesis process, the bidirectional crosstalk between epithelial cells and the surrounding stroma can activate resident fibroblasts, driving cancer development and progression [27, 85]. In this intricate interplay, CAFs may reshape the TME by secreting growth factors, pro-inflammatory molecules and other mediators, which in turn generate a permissive environment leading to cancer cell invasion and migration, angiogenesis, recruitment of inflammatory cells, modulation of immune responses and remodeling of the extracellular matrix (ECM) [27, 86]. In line with these autocrine-paracrine loops occurring between cancer cells and CAFs, we revealed that the CAFs-like cells derived from the IL-1β/IL1R1 stimulation of normal fibroblasts contribute to the growth and migration capabilities of TNBC cells.

Conclusions

Here, we have provided novel evidence showing that the IGF1R/DDR1/GPER axis orchestrates IL-1β induction and secretion in response to IGF1 exposure in TNBC cells. Furthermore, our study sheds light on the role of IL-1β signaling in promoting a proliferative and motile tumor niche that facilitates cancer progression. Collectively, these findings suggest that IL-1β may represent a potential target in more comprehensive therapeutic strategies in TNBC patients, particularly in obese subjects characterized by high IGF1 levels. Importantly, the IGF1/IL-1β network may also serve as a diagnostic and prognostic biomarker for identifying TNBC patients showing an aggressive phenotype. These observations underscore the importance of patient stratification for designing personalized therapeutic strategies targeting tumor-stroma interactions and obesity-associated inflammatory responses within the TNBC microenvironment.

Supplementary Information

The online version contains supplementary material available at https://doi.org/10.1186/s12967-025-06730-w.

Additional file 1.

Additional file 2.

Additional file 3.

Acknowledgements
Not applicable.

Author contributions
DS designed the study, performed the experiments and analyzed data. MT performed the bioinformatic analysis and analyzed data. FC, AZ, SDR, MDD, FS, CM and AAM performed experiments. AMM and CC provided samples. EMDF and AB revised the manuscript. MM and RL designed the study, analyzed data and wrote the manuscript. All authors reviewed and edited the final manuscript.

Funding
Fondazione AIRC supported RL (IG n. 27386), AB (IG n. 23369) and EMDF (Start-Up Grant 21651). Ministero della Salute (Italy) supported AB, RL and MM (RF-2019–12368937). Ministero dell'Università e Ricerca supported AB (Prin 2022 2022Y79PT4), EMDF (Prin 2022 PNRR P2022MALRP), RL (Prin 2022 202282CMEA; Prin 2022 PNRR P2022MALRP) and MM (Prin 2022 2022Y79PT4).

This work was also funded by: (1) The Next Generation EU—project Tech4You—n. ECS0000009; (2) The National Plan for NRRP Complementary Investments - project n. PNC0000003 - AdvaNced Technologies for Human-centrEd Medicine (ANTHEM); (3) The Next Generation EU—Project Age-It: "Ageing Well in an Ageing Society" [DM 1557 11.10.2022]; (4) POS RADIOAM-ICA project funded by the Italian Minister of Health (CUP: H53C22000650006); (5) POS CAL.HUB.RIA project funded by the Italian Minister of Health (CUP H53C22000800006); (6) Proof of Concept (PoC)—Patent Enhancement Program Unical Pathways (UP) (CUP C28H23000330002); (7) BAC PNRR UniMI—Advances in Extracellular Vesicles membrane fusion processes for enhanced loading of genetic materials ADEVEGLIO (DR 3926/06.06.2024); (8) BAC PNRR—Innovative Design and Synthesis of Lipid Nanocarriers for Targeted Gene Delivery (LIPGENOMIX).

Availability of data and materials
All data generated or analyzed during this study are included in this published article and its supplementary information files. Any additional information required to reanalyze the data reported in this paper is available from the corresponding author upon reasonable request.

Declarations

Ethics approval and consent to participate
Not applicable.

Consent for publication
Not applicable.

Competing interests
The authors declare that they have no competing interests.

Author details
[1]Department of Pharmacy, Health and Nutritional Sciences, University of Calabria, 87036 Rende, Italy. [2]Department of Medicine and Surgery, University of Enna "Kore", 94100 Enna, Italy. [3]Breast and General Surgery Unit, Annunziata Hospital Cosenza, 87100 Cosenza, Italy. [4]Complex Operative Oncology Unit, Annunziata Hospital Cosenza, 87100 Cosenza, Italy. [5]Endocrinology, Department of Clinical and Experimental Medicine, University of Catania, Garibaldi-Nesima Hospital, 95122 Catania, Italy.

Received: 22 May 2025 Accepted: 6 June 2025
Published online: 17 June 2025

References

1. Nguyen H-L, Geukens T, Maetens M, Aparicio S, Bassez A, Borg A, et al. Obesity-associated changes in molecular biology of primary breast cancer. Nat Commun. 2023;14:4418.
2. Picon-Ruiz M, Morata-Tarifa C, Valle-Goffin JJ, Friedman ER, Slingerland JM. Obesity and adverse breast cancer risk and outcome: Mechanistic insights and strategies for intervention. CA Cancer J Clin. 2017;67:378–97.
3. Schleh MW, Caslin HL, Garcia JN, Mashayekhi M, Srivastava G, Bradley AB, et al. Metaflammation in obesity and its therapeutic targeting. Sci Transl Med. 2023;15:9382.
4. Jin X, Qiu T, Li L, Yu R, Chen X, Li C, et al. Pathophysiology of obesity and its associated diseases. Acta Pharm Sin B. 2023;13:2403–24.
5. Brown KA. Metabolic pathways in obesity-related breast cancer. Nat Rev Endocrinol. 2021;17:350–63.
6. Bousquenaud M, Fico F, Solinas G, Rüegg C, Santamaria-Martínez A. Obesity promotes the expansion of metastasis-initiating cells in breast cancer. Breast Cancer Res. 2018;20:104.
7. Lehuédé C, Li X, Dauvillier S, Vaysse C, Franchet C, Clement E, et al. Adipocytes promote breast cancer resistance to chemotherapy, a process amplified by obesity: role of the major vault protein (MVP). Breast Cancer Res. 2019;21:7.
8. Newport-Ratiu PA, Hussein KA, Carter T, Panjarian S, Jonnalagadda SC, Pandey MK. Unveiling the intricate dance: Obesity and TNBC connection examined. Life Sci. 2024;357: 123082.
9. Endogenous Hormones and Breast Cancer Collaborative Group, Key TJ, Appleby PN, Reeves GK, Roddam AW. Insulin-like growth factor 1 (IGF1), IGF binding protein 3 (IGFBP3), and breast cancer risk: pooled individual data analysis of 17 prospective studies. Lancet Oncol. 2010;11:530–42.
10. Lega IC, Lipscombe LL. Review: diabetes, obesity, and cancer-pathophysiology and clinical implications. Endocr Rev. 2020;41:33–52.
11. Kubo H, Sawada S, Satoh M, Asai Y, Kodama S, Sato T, et al. Insulin-like growth factor-1 levels are associated with high comorbidity of metabolic disorders in obese subjects; a Japanese single-center, retrospective-study. Sci Rep. 2022;12:20130.
12. Perry RJ, Shulman GI. Mechanistic links between obesity, insulin, and cancer. Trends Cancer. 2020;6:75–8.
13. Morrione A, Belfiore A. Obesity, diabetes, and cancer: the role of the insulin/IGF axis. Mech Clin Implic Biomol. 2022;12:612.
14. Law JH, Habibi G, Hu K, Masoudi H, Wang MYC, Stratford AL, et al. Phosphorylated insulin-like growth factor-i/insulin receptor is present in all breast cancer subtypes and is related to poor survival. Cancer Res. 2008;68:10238–46.
15. Christopoulos PF, Msaouel P, Koutsilieris M. The role of the insulin-like growth factor-1 system in breast cancer. Mol Cancer. 2015;14:43.
16. Rigiracciolo DC, Nohata N, Lappano R, Cirillo F, Talia M, Scordamaglia D, et al. IGF-1/IGF-1R/FAK/YAP Transduction Signaling Prompts Growth Effects in Triple-Negative Breast Cancer (TNBC) Cells. Cells. 2020. https://doi.org/10.3390/cells9041010.
17. De Francesco EM, Sims AH, Maggiolini M, Sotgia F, Lisanti MP, Clarke RB. GPER mediates the angiocrine actions induced by IGF1 through the HIF-1α/VEGF pathway in the breast tumor microenvironment. Breast Cancer Res. 2017;19:129.
18. De Marco P, Bartella V, Vivacqua A, Lappano R, Santolla MF, Morcavallo A, et al. Insulin-like growth factor-I regulates GPER expression and function in cancer cells. Oncogene. 2013;32:678–88.
19. Muoio MG, Talia M, Lappano R, Sims AH, Vella V, Cirillo F, et al. Activation of the S100A7/RAGE Pathway by IGF-1 Contributes to Angiogenesis in Breast Cancer. Cancers. 2021. https://doi.org/10.3390/cancers13040621.
20. Ter Braak B, Siezen CL, Lee JS, Rao P, Voorhoeve C, Ruppin E, et al. Insulin-like growth factor 1 receptor activation promotes mammary gland tumor development by increasing glycolysis and promoting biomass production. Breast Cancer Res. 2017;19:14.
21. Avino S, De Marco P, Cirillo F, Santolla MF, De Francesco EM, Perri MG, et al. Stimulatory actions of IGF-I are mediated by IGF-IR cross-talk with GPER and DDR1 in mesothelioma and lung cancer cells. Oncotarget. 2016;7:52710–28.
22. Vella V, Giuliano M, Nicolosi ML, Majorana MG, Marć MA, Muoio MG, et al. DDR1 affects metabolic reprogramming in breast cancer cells by cross-talking to the insulin/IGF system. Biomolecules. 2021;11:926.
23. Belfiore A, Malaguarnera R, Nicolosi ML, Lappano R, Ragusa M, Morrione A, et al. A novel functional crosstalk between DDR1 and the IGF axis and its relevance for breast cancer. Cell Adh Migr. 2018;12:305–14.
24. Yuan J, Liu M, Yang L, Tu G, Zhu Q, Chen M, et al. Acquisition of epithelial-mesenchymal transition phenotype in the tamoxifen-resistant breast cancer cell: a new role for G protein-coupled estrogen receptor in mediating tamoxifen resistance through cancer-associated fibroblast-derived fibronectin and β1-integrin signaling pathway in tumor cells. Breast Cancer Res. 2015;17:69.
25. Lappano R, Santolla MF, Pupo M, Sinicropi MS, Caruso A, Rosano C, et al. MIBE acts as antagonist ligand of both estrogen receptor α and GPER in breast cancer cells. Breast Cancer Res. 2012;14:R12.
26. De Francesco EM, Lappano R, Santolla MF, Marsico S, Caruso A, Maggiolini M. HIF-1α/GPER signaling mediates the expression of VEGF induced by hypoxia in breast cancer associated fibroblasts (CAFs). Breast Cancer Res. 2013;15:R64.
27. Lappano R, Rigiracciolo DC, Belfiore A, Maggiolini M, De Francesco EM. Cancer associated fibroblasts: role in breast cancer and potential as therapeutic targets. Expert Opin Ther Targets. 2020;24:559–72.
28. Yuan J, Yang L, Li Z, Zhang H, Wang Q, Huang J, et al. The role of the tumor microenvironment in endocrine therapy resistance in hormone receptor-positive breast cancer. Front Endocrinol (Lausanne). 2023;14:1261283.

29. Vella V, Lappano R, Bonavita E, Maggiolini M, Clarke RB, Belfiore A, et al. Insulin/IGF axis and the Receptor for Advanced Glycation End Products: role in meta-inflammation and potential in cancer therapy. Endocr Rev. 2023. https://doi.org/10.1210/endrev/bnad005.
30. Kunnumakkara AB, Sailo BL, Banik K, Harsha C, Prasad S, Gupta SC, et al. Chronic diseases, inflammation, and spices: how are they linked? J Transl Med. 2018;16:14.
31. Hu D, Li Z, Zheng B, Lin X, Pan Y, Gong P, et al. Cancer-associated fibroblasts in breast cancer: challenges and opportunities. Cancer Commun. 2022;42:401–34.
32. Zhao H, Wu L, Yan G, Chen Y, Zhou M, Wu Y, et al. Inflammation and tumor progression: signaling pathways and targeted intervention. Signal Transduct Target Ther. 2021;6:263.
33. Balkwill F. Cancer and the chemokine network. Nat Rev Cancer. 2004;4:540–50.
34. Lappano R, Talia M, Cirillo F, Rigiracciolo DC, Scordamaglia D, Guzzi R, et al. The IL1β-IL1R signaling is involved in the stimulatory effects triggered by hypoxia in breast cancer cells and cancer-associated fibroblasts (CAFs). J Exp Clin Cancer Res. 2020;39:153.
35. Kaplanov I, Carmi Y, Kornetsky R, Shemesh A, Shurin GV, Shurin MR, et al. Blocking IL-1β reverses the immunosuppression in mouse breast cancer and synergizes with anti-PD-1 for tumor abrogation. Proc Natl Acad Sci U S A. 2019;116:1361–9.
36. Lewis AM, Varghese S, Xu H, Alexander HR. Interleukin-1 and cancer progression: the emerging role of interleukin-1 receptor antagonist as a novel therapeutic agent in cancer treatment. J Transl Med. 2006;4:48.
37. Chavey C, Bibeau F, Gourgou-Bourgade S, Burlinchon S, Boissière F, Laune D, et al. Oestrogen receptor negative breast cancers exhibit high cytokine content. Breast Cancer Res. 2007;9:R15.
38. Jin L, Yuan RQ, Fuchs A, Yao Y, Joseph A, Schwall R, et al. Expression of interleukin-1beta in human breast carcinoma. Cancer. 1997;80:421–34.
39. Ciriello G, Gatza ML, Beck AH, Wilkerson MD, Rhie SK, Pastore A, et al. Comprehensive molecular portraits of invasive lobular breast cancer. Cell. 2015;163:506–19.
40. Pearce DA, Nirmal AJ, Freeman TC, Sims AH. Continuous Biomarker Assessment by Exhaustive Survival Analysis [Internet]. bioRxiv. 2018 [cited 2023 Mar 8]. p. 208660. Available from: https://www.biorxiv.org/content/https://doi.org/10.1101/208660v2
41. Talia M, Cirillo F, Spinelli A, Zicarelli A, Scordamaglia D, Muglia L, et al. The Ephrin tyrosine kinase a3 (EphA3) is a novel mediator of RAGE-prompted motility of breast cancer cells. J Exp Clin Cancer Res. 2023;42:164.
42. Cirillo F, Spinelli A, Talia M, Scordamaglia D, Santolla MF, Grande F, et al. Estetrol/GPER/SERPINB2 transduction signaling inhibits the motility of triple-negative breast cancer cells. J Transl Med. 2024;22:450.
43. Malaguarnera R, Nicolosi ML, Sacco A, Morcavallo A, Vella V, Voci C, et al. Novel cross talk between IGF-IR and DDR1 regulates IGF-IR trafficking, signaling and biological responses. Oncotarget. 2015;6:16084–105.
44. Cirillo F, Talia M, Santolla MF, Pellegrino M, Scordamaglia D, Spinelli A, et al. GPER deletion triggers inhibitory effects in triple negative breast cancer (TNBC) cells through the JNK/c-Jun/p53/Noxa transduction pathway. Cell Death Discov. 2023;9:353.
45. Khodabakhshaghdam S, Khoshfetrat AB, Rahbarghazi R. Alginate-chitosan core-shell microcapsule cultures of hepatic cells in a small scale stirred bioreactor: impact of shear forces and microcapsule core composition. J Biol Eng. 2021;15:14.
46. Scordamaglia D, Cirillo F, Talia M, Santolla MF, Rigiracciolo DC, Muglia L, et al. Metformin counteracts stimulatory effects induced by insulin in primary breast cancer cells. J Transl Med. 2022;20:263.
47. Yan B, Huang M, Zeng C, Yao N, Zhang J, Yan B, et al. Locally produced IGF-1 promotes hypertrophy of the ligamentum flavum via the mTORC1 signaling pathway. Cell Physiol Biochem. 2018;48:293–303.
48. Blackstock CD, Higashi Y, Sukhanov S, Shai S-Y, Stefanovic B, Tabony AM, et al. Insulin-like growth factor-1 increases synthesis of collagen type I via induction of the mRNA-binding protein LARP6 expression and binding to the 5′ stem-loop of COL1a1 and COL1a2 mRNA. J Biol Chem. 2014;289:7264–74.
49. Chen X, Ma C, Li Y, Liang Y, Chen T, Han D, et al. COL5A1 promotes triple-negative breast cancer progression by activating tumor cell-macrophage crosstalk. Oncogene. 2024;43:1742–56.
50. Li X, Jin Y, Xue J. Unveiling collagen's role in breast cancer: Insights into expression patterns, functions and clinical implications. Int J Gen Med. 2024;17:1773–87.
51. Gao H, Tian Q, Zhou Y, Zhu L, Lu Y, Ma Y, et al. 3D collagen fiber concentration regulates Treg cell infiltration in triple negative breast cancer. Front Immunol. 2022;13: 904418.
52. Belfiore A, Frasca F, Pandini G, Sciacca L, Vigneri R. Insulin receptor isoforms and insulin receptor/insulin-like growth factor receptor hybrids in physiology and disease. Endocr Rev. 2009;30:586–623.
53. Xu S, Xu H, Wang W, Li S, Li H, Li T, et al. The role of collagen in cancer: from bench to bedside. J Transl Med. 2019;17:309.
54. Chen P, Cescon M, Bonaldo P. Collagen VI in cancer and its biological mechanisms. Trends Mol Med. 2013;19:410–7.
55. Iyengar P, Combs TP, Shah SJ, Gouon-Evans V, Pollard JW, Albanese C, et al. Adipocyte-secreted factors synergistically promote mammary tumorigenesis through induction of anti-apoptotic transcriptional programs and proto-oncogene stabilization. Oncogene. 2003;22:6408–23.
56. Wishart AL, Conner SJ, Guarin JR, Fatherree JP, Peng Y, McGinn RA, et al. Decellularized extracellular matrix scaffolds identify full-length collagen VI as a driver of breast cancer cell invasion in obesity and metastasis. Sci Adv. 2020;6:3175.
57. Iyengar P, Espina V, Williams TW, Lin Y, Berry D, Jelicks LA, et al. Adipocyte-derived collagen VI affects early mammary tumor progression in vivo, demonstrating a critical interaction in the tumor/stroma microenvironment. J Clin Invest. 2005;115:1163–76.
58. Abdulhussein R, McFadden C, Fuentes-Prior P, Vogel WF. Exploring the collagen-binding site of the DDR1 tyrosine kinase receptor. J Biol Chem. 2004;279:31462–70.
59. Vogel W, Gish GD, Alves F, Pawson T. The discoidin domain receptor tyrosine kinases are activated by collagen. Mol Cell. 1997;1:13–23.
60. Elaraj DM, Weinreich DM, Varghese S, Puhlmann M, Hewitt SM, Carroll NM, et al. The role of interleukin 1 in growth and metastasis of human cancer xenografts. Clin Cancer Res. 2006;12:1088–96.
61. Wu T-C, Xu K, Martinek J, Young RR, Banchereau R, George J, et al. IL1 receptor antagonist controls transcriptional signature of inflammation in patients with metastatic breast cancer. Cancer Res. 2018;78:5243–58.
62. De Marco P, Lappano R, De Francesco EM, Cirillo F, Pupo M, Avino S, et al. GPER signalling in both cancer-associated fibroblasts and breast cancer cells mediates a feedforward IL1β/IL1R1 response. Sci Rep. 2016;6:24354.
63. Xu H, Tan M, Hou G-Q, Sang Y-Z, Lin L, Gan X-C, et al. Blockade of DDR1/PYK2/ERK signaling suggesting SH2 superbinder as a novel autophagy inhibitor for pancreatic cancer. Cell Death Dis. 2023;14:811.
64. Monje P, Hernández-Losa J, Lyons RJ, Castellone MD, Gutkind JS. Regulation of the transcriptional activity of c-Fos by ERK. A novel role for the prolyl isomerase PIN1. J Biol Chem. 2005;280:35081–4.
65. Sahai E, Astsaturov I, Cukierman E, DeNardo DG, Egeblad M, Evans RM, et al. A framework for advancing our understanding of cancer-associated fibroblasts. Nat Rev Cancer. 2020;20:174–86.
66. Hanahan D, Coussens LM. Accessories to the crime: functions of cells recruited to the tumor microenvironment. Cancer Cell. 2012;21:309–22.
67. Nurmik M, Ullmann P, Rodriguez F, Haan S, Letellier E. In search of definitions: Cancer-associated fibroblasts and their markers. Int J Cancer. 2020;146:895–905.
68. Kim HM, Jung WH, Koo JS. Expression of cancer-associated fibroblast related proteins in metastatic breast cancer: an immunohistochemical analysis. J Transl Med. 2015;13:222.
69. Hanahan D. Hallmarks of cancer: New dimensions. Cancer Discov. 2022;12:31–46.
70. Grivennikov SI, Greten FR, Karin M. Immunity, inflammation, and cancer. Cell. 2010;140:883–99.
71. Esser N, Legrand-Poels S, Piette J, Scheen AJ, Paquot N. Inflammation as a link between obesity, metabolic syndrome and type 2 diabetes. Diabetes Res Clin Pract. 2014;105:141–50.
72. Hanahan D, Weinberg RA. Hallmarks of cancer: the next generation. Cell. 2011;144:646–74.
73. Ben-Baruch A. Host microenvironment in breast cancer development: inflammatory cells, cytokines and chemokines in breast cancer progression: reciprocal tumor-microenvironment interactions. Breast Cancer Res. 2003;5:31–6.
74. Kolb R, Sutterwala FS, Zhang W. Obesity and cancer: inflammation bridges the two. Curr Opin Pharmacol. 2016;29:77–89.

75. Fasshauer M, Blüher M. Adipokines in health and disease. Trends Pharmacol Sci. 2015;36:461–70.
76. Chawla A, Nguyen KD, Goh YPS. Macrophage-mediated inflammation in metabolic disease. Nat Rev Immunol. 2011;11:738–49.
77. Mantovani A, Barajon I, Garlanda C. IL-1 and IL-1 regulatory pathways in cancer progression and therapy. Immunol Rev. 2018;281:57–61.
78. Voronov E, Shouval DS, Krelin Y, Cagnano E, Benharroch D, Iwakura Y, et al. IL-1 is required for tumor invasiveness and angiogenesis. Proc Natl Acad Sci U S A. 2003;100:2645–50.
79. Maker AV, Katabi N, Qin L-X, Klimstra DS, Schattner M, Brennan MF, et al. Cyst fluid interleukin-1beta (IL1beta) levels predict the risk of carcinoma in intraductal papillary mucinous neoplasms of the pancreas. Clin Cancer Res. 2011;17:1502–8.
80. Zhou J, Tulotta C, Ottewell PD. IL-1β in breast cancer bone metastasis. Expert Rev Mol Med. 2022;24: e11.
81. Bota-Rabassedas N, Banerjee P, Niu Y, Cao W, Luo J, Xi Y, et al. Contextual cues from cancer cells govern cancer-associated fibroblast heterogeneity. Cell Rep. 2021;35: 109009.
82. Li Q, Lv X, Han C, Kong Y, Dai Z, Huo D, et al. Enhancer reprogramming promotes the activation of cancer-associated fibroblasts and breast cancer metastasis. Theranostics. 2022;12:7491–508.
83. Cazet AS, Hui MN, Elsworth BL, Wu SZ, Roden D, Chan C-L, et al. Targeting stromal remodeling and cancer stem cell plasticity overcomes chemoresistance in triple negative breast cancer. Nat Commun. 2018;9:2897.
84. Sharon Y, Raz Y, Cohen N, Ben-Shmuel A, Schwartz H, Geiger T, et al. Tumor-derived osteopontin reprograms normal mammary fibroblasts to promote inflammation and tumor growth in breast cancer. Cancer Res. 2015;75:963–73.
85. Zhang W, Wang J, Liu C, Li Y, Sun C, Wu J, et al. Crosstalk and plasticity driving between cancer-associated fibroblasts and tumor microenvironment: significance of breast cancer metastasis. J Transl Med. 2023;21:827.
86. Zhou S, Zhao Z, Wang Z, Xu H, Li Y, Xu K, et al. Cancer-associated fibroblasts in carcinogenesis. J Transl Med. 2025;23:50.

Publisher's Note